

Diagrammatic approach to soft non-Abelian dynamics at high temperature

Dietrich Bödeker ¹

The Niels Bohr Institute, Blegdamsvej 17, DK-2100 Copenhagen Ø, Denmark

Abstract

The dynamics of soft ($|\mathbf{p}| \sim g^2 T$) non-Abelian gauge fields at finite temperature is non-perturbative. The effective theory for the soft scale is determined by diagrams with external momenta $p_0 \lesssim g^2 T$, $|\mathbf{p}| \sim g^2 T$ and loop momenta larger than $g^2 T$. We consider the polarization tensor beyond the hard thermal loop approximation, which accounts for loop momenta of order T . There are higher loop diagrams, involving also the scale gT , which are as important as the hard thermal loops. These higher loop contributions are characteristic for non-Abelian gauge theories and their calculation is simplified by using the hard thermal loop effective theory. Remarkably, the effective one-loop polarization tensor is found to be gauge fixing independent and transverse at leading order in g . The transversality indicates that this approach leads to a gauge invariant effective theory.

PACS numbers: 11.10.Wx, 11.15.-q

¹e-mail: bodeker@nbi.dk

1 Introduction

Even at very high temperatures, when the running gauge coupling g is small, perturbation theory for non-Abelian gauge theories breaks down at the spatial momentum scale g^2T [1, 2]. For static quantities, like the free energy or correlation lengths, one can integrate out the high momentum modes² ($p \gg g^2T$) in perturbation theory using dimensional reduction [3, 4]. Then, at leading order, the non-perturbative physics associated with the scale g^2T is described by a 3-dimensional Euclidean gauge theory, which can be easily treated in lattice simulations.

Dynamical quantities, which are sensitive to the scale g^2T , are more difficult to deal with. Since one has to consider non-zero real frequencies, one cannot use dimensional reduction. A prominent example for such a quantity is the rate for electroweak baryon number violation³, which, at leading order, is entirely due to gauge field modes with spatial momenta of order g^2T [6].

Fortunately, even for non-zero p_0 , one can use perturbation theory to integrate out high momentum degrees of freedom to obtain an effective theory for the soft field modes. At leading logarithmic order, this effective theory is described by a Langevin equation [7]. It determines the characteristic frequency of the soft field modes as

$$p_0 \sim g^4T \log(1/g), \quad (1.1)$$

and it allows for a lattice calculation of the baryon number violation rate [8].

The most direct approach to such an effective theory is to compute diagrams for soft external momenta, while the loop momenta are restricted to be larger than g^2T . At one-loop order, the dominant contributions are the so-called hard thermal loops [9], which are saturated by loop momenta of order T . They lead to the Debye-screening of electric interactions on the length scale $1/(gT)$. Therefore, only the magnetic degrees of freedom are non-perturbative.

For a long time it was assumed, that the characteristic frequency of the soft magnetic modes is of order g^2T . It was realized in Ref. [10], that hard thermal loops drastically change this picture. They lead to a strong (Landau-) damping of the soft, non-perturbative dynamics. Considering the hard thermal loop resummed propagator, the characteristic frequency of the soft magnetic modes can be estimated as $p_0 \sim g^4T$ [10].

In this paper, we investigate the polarization tensor for soft external momenta beyond the hard thermal loop approximation. There are higher loop contributions, which are

²For spatial vectors I use the notation $k = |\mathbf{k}|$. 4-momentum vectors are denoted by $K^\mu = (k^0, \mathbf{k})$, and the metric has the signature $(+ - - -)$.

³More precisely, the Chern-Simons number diffusion rate, which is proportional to the baryon number violation rate close to thermal equilibrium [5].

not suppressed relative to the hard thermal loops. They consist of self energy insertions on the hard loops and of ladder-type diagrams, and they can be economically calculated using the hard thermal loop effective theory. This paper describes the calculation of the effective one-loop polarization tensor, the leading logarithmic result was presented in [11]. Summing the leading logarithmic contributions from all n -loop diagrams by solving a Boltzmann equation for the soft field modes, one obtains the effective theory of Ref. [7]. Recently, this effective theory has also been obtained in [12], the Boltzmann equation was also obtained in [12]-[14]. A recent detailed derivation of the Boltzmann equation can be found in [15].

The paper is organized as follows: Sect. 2 briefly reviews some properties of hard thermal loops. Sect. 3 discusses higher loop contributions to the polarization tensor, which can be as large as the hard thermal loops. Sect. 4 contains the calculation of the one-loop polarization tensor within the hard thermal loop effective theory in a covariant gauge. The results are summarized and discussed in Sect. 5. Appendix A contains the expression for the sum over Matsubara frequencies which is used in the main text. Finally, it is shown in Appendix B, that the results of Sect. 4 are also valid in Coulomb-like gauges.

2 Hard thermal loops

Hard thermal loops are one-loop contributions to n -point functions for external momenta small compared to T . They are saturated by loop momenta of order T . Furthermore, the dominant contribution is obtained when one momentum in the loop is on shell, $Q^2 = 0$. For remaining propagators containing Q , one can use a large energy, or eikonal approximation

$$\frac{1}{(Q + P)^2} \simeq \frac{1}{2q} \frac{1}{v \cdot P} , \quad (2.1)$$

where P is some linear combination of the external momenta, and $v^\mu = Q^\mu/q$. The spatial part of v is the velocity of the hard particles in the rest frame of the plasma. Due to Eq. (2.1), the angular integration over \mathbf{v} and the integration over q factorize.

The hard thermal loop 2-point function, which is the same in Abelian and non-Abelian theories, reads [16]

$$\delta\Pi_{\mu\nu}(P) = m_D^2 \left[-g_{\mu 0} g_{\nu 0} + p_0 \int \frac{d\Omega_{\mathbf{v}}}{4\pi} \frac{v_\mu v_\nu}{v \cdot P} \right]. \quad (2.2)$$

The q -integration is responsible for the factor m_D^2 , which is the leading order Debye mass squared. All fields coupling to the gauge fields contribute to the hard thermal

loops in the same functional form. In a $SU(N)$ gauge theory with N_f fermions and N_s scalars in the fundamental representation one has $m_D^2 = (1/3)(N + N_s/2 + N_f/2)g^2T^2$. Finally, the integral $\int d\Omega_{\mathbf{v}}$ is over the orientation of the unit vector \mathbf{v} .

Since (2.2) is transverse,

$$p^\mu \delta\Pi_{\mu\nu}(P) = 0, \quad (2.3)$$

it can be written in terms of the 3-dimensionally (3-d) transverse and longitudinal projectors [16]⁴

$$\mathcal{P}_t^{ij}(\mathbf{p}) = \delta^{ij} - \frac{p^i p^j}{p^2}, \quad \mathcal{P}_t^{\mu 0}(\mathbf{p}) = 0, \quad (2.4)$$

$$\mathcal{P}_\ell^{\mu\nu}(P) = \frac{p^\mu p^\nu}{P^2} - g^{\mu\nu} - \mathcal{P}_t^{\mu\nu}(\mathbf{p}). \quad (2.5)$$

such that

$$\delta\Pi^{\mu\nu}(P) = \mathcal{P}_t^{\mu\nu}(\mathbf{p})\delta\Pi_t(P) + \mathcal{P}_\ell^{\mu\nu}(P)\delta\Pi_\ell(P). \quad (2.6)$$

For momenta $p_0, p \lesssim gT$, the hard thermal loop (2.2) cannot be considered as a small correction to the tree level kinetic term, and it has to be resummed. In a covariant gauge with gauge fixing parameter ξ , the resummed propagator reads [16]

$$\Delta^{\mu\nu}(P) = \mathcal{P}_t^{\mu\nu}(\mathbf{p})\Delta_t(P) + \mathcal{P}_\ell^{\mu\nu}(P)\Delta_\ell(P) + \xi \frac{p^\mu p^\nu}{P^4}. \quad (2.7)$$

The 3-d transverse and longitudinal propagators

$$\Delta_{t,\ell}(P) = \frac{1}{-P^2 + \delta\Pi_{t,\ell}(P)}. \quad (2.8)$$

have poles at $p_0^2 = \omega_{t,\ell}^2(p) > p^2$, and they have a cut for $P^2 < 0$.

For static quantities, like the free energy or equal time correlation functions, it is convenient to work in the imaginary time formalism. Then p_0 is an imaginary Matsubara frequency, and for $p \lesssim gT$ the dominant contribution is given by the $p_0 = 0$ modes. In this case the 3-d transverse fields are unaffected by hard thermal loops, $\delta\Pi_t(0, \mathbf{p}) = 0$, and the only effect of hard thermal loops is the Debye screening of the longitudinal fields due to $\delta\Pi_\ell(0, \mathbf{p}) = m_D^2$.

For dynamical quantities p_0 has to be analytically continued towards the real axis. Different ways of approaching the real axis correspond to different time ordering prescriptions. For definiteness, in this paper we will consider the case that

$$p_0 = \text{Re}(p_0) + i\epsilon, \quad (2.9)$$

⁴Note that the projectors in Eqs. (2.4), (2.5) have a sign different from the ones in Ref. [16].

which gives the retarded propagator.

When p_0 is non-zero, also the magnetic, or 3-d transverse fields are screened (“dynamical screening”). For $p \sim g^2 T$ this has a dramatic effect [10], since $\Delta_t(P)$ is smaller than the free propagator by two powers of g when $p_0 \sim g^2 T$. Therefore the transverse gauge fields perform only small fluctuations for this frequency scale. In order to obtain large fluctuations⁵, which are necessary for non-perturbative processes like electroweak baryon number violation, one has to consider the small frequency limit $p_0 \ll p$, in which case

$$\delta\Pi_t(P) \simeq -i\frac{\pi}{4}m_D^2\frac{p_0}{p} \quad (p_0 \ll p). \quad (2.10)$$

Then the hard thermal loop resummed propagator becomes

$$\Delta_t(P) \simeq \frac{1}{p^2} \frac{i\gamma_p}{p_0 + i\gamma_p} \quad (p_0 \ll p), \quad (2.11)$$

where $\gamma_p = 4p^3/(\pi m_D^2)$. Since γ_p is of order $g^4 T$ when $p \sim g^2 T$, Eq. (2.11) indicates that the characteristic frequency for the soft transverse modes is $p_0 \sim g^4 T$ [10]. The higher loop contributions discussed in this paper lead to a logarithmic correction to this estimate.

3 Beyond hard thermal loops

It will now become clear, that the hard thermal loop approximation is not sufficient for obtaining the correct effective theory for the soft modes. Consider a hard thermal loop and imagine adding a self energy insertion on an internal line, where the additional loop momentum K is of order gT . This gives the diagram in Fig. 1(a), in which the hard loop momentum Q is on shell, $Q^2 = 0$. Since the external momentum P is soft, the momentum $Q + P$ is almost on shell.

Compared to $\delta\Pi$, the diagram in Fig. 1(a) contains two additional vertices, each of order $gq \sim gT$. There are two additional propagators containing the hard momentum Q , for which one can make the eikonal approximation (2.1), and there is one hard thermal loop resummed propagator $\Delta(K) \sim 1/(g^2 T^2)$. The loop integral over K comes with a Bose distribution function

$$n(k_0) = \frac{1}{e^{k_0/T} - 1}, \quad (3.1)$$

which can be approximated as $n(k_0) \simeq T/k_0$. Thus we can estimate

$$\Pi^{(1a)}(P) \sim \delta\Pi(P) \times \left(g^2 T^2\right) \left(\int_{k \sim gT} d^4 k \frac{T}{k_0}\right) \left(\frac{1}{T} \frac{1}{v \cdot P}\right) \left(\frac{1}{T} \frac{1}{v \cdot (K + P)}\right) \Delta(K)$$

⁵For an instructive discussion, see [10].

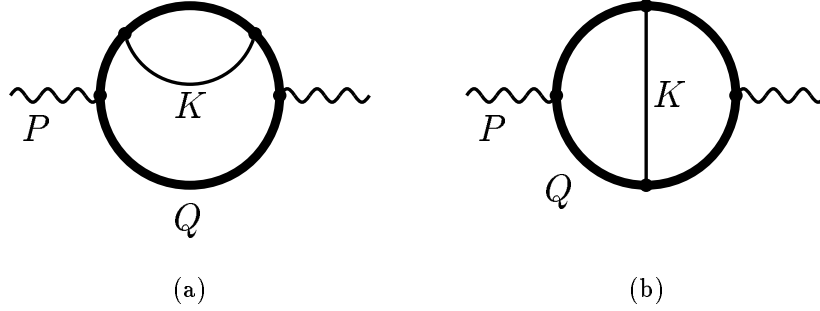


Figure 1: Two-loop contribution to the polarization tensor. The external momentum P is soft ($p_0, p \lesssim g^2 T$) and the momentum Q is hard ($q_0, q \sim T$). The thick lines denote propagators with momenta of order T . The thin lines are hard thermal loop resummed gauge field propagators $\Delta(K)$ with $k_0, k \sim gT$.

$$\sim \delta\Pi(P) \times \frac{g^2 T}{v \cdot P}. \quad (3.2)$$

This shows that the diagram in Fig. 1(a) can be as large as $\delta\Pi(P)$, when p_0 and p are of order $g^2 T$ or smaller.

Now consider the diagram in Fig. 1(b). Proceeding as above we estimate

$$\Pi^{(1b)}(P) \sim \delta\Pi(P) \times \left(g^2 T^2\right) \left(\int_{k \sim gT} d^4 k \frac{T}{k_0}\right) \left(\frac{1}{T} \frac{1}{v \cdot K}\right) \left(\frac{1}{T} \frac{1}{v \cdot (K + P)}\right) \Delta(K). \quad (3.3)$$

On first sight, this diagram appears to be smaller than (3.2), since one eikonal propagator $1/(v \cdot P)$ got replaced by $1/(v \cdot K)$. However, performing the integral over k_0 , one obtains contributions from the poles of the propagators. For example, at the pole $k_0 = \mathbf{v} \cdot \mathbf{k}$, the second propagator in (3.3) turns into $1/(v \cdot P)$. Therefore we can estimate

$$\begin{aligned} \Pi^{(1b)}(P) &\sim \delta\Pi(P) \times \left(g^2 T^2\right) \left(\int_{k \sim gT} d^3 k \frac{1}{k}\right) \left(\frac{1}{T} \frac{1}{v \cdot P}\right) \Delta(K) \\ &\sim \delta\Pi(P) \times \frac{g^2 T}{v \cdot P}, \end{aligned} \quad (3.4)$$

which is as large as Eq. (3.2).

The above estimates for the diagrams in Fig. 1 are well known and have been discussed extensively in the literature [17, 18, 19]. In order to deal with these large contributions, the right half of diagram 1(b), together with the propagator $\Delta(K)$ has been interpreted as an insertion of a vertex correction. Then higher loop contributions were summed using a Schwinger-Dyson equation. For Abelian theories it was found that the large corrections cancel in the final answer.

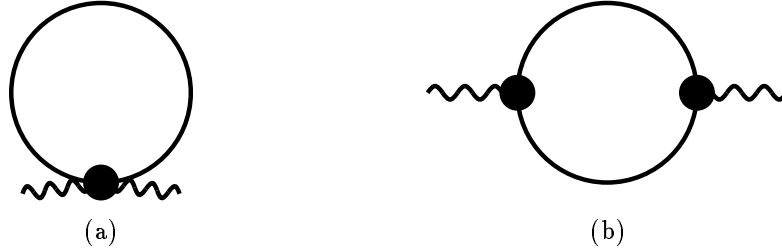


Figure 2: One-loop contributions to the polarization tensor in the hard thermal loop effective theory. The heavy dots are hard thermal loop vertices. Otherwise the notation is the same as in Fig. 1.

It should be emphasized that this view is not convenient, because it obscures the nature of the cancellation mechanism. Let us look at the diagrams from a different perspective [11]. Imagine first doing the integration over the hard momentum Q , with K kept fixed. This corresponds to integrating out hard momenta to obtain an effective 4-point vertex for momenta small compared to T . Now we can make use of a well known fact: In an Abelian theory there are no hard thermal loop vertices for gauge fields only. In other words, the large contributions due to the diagrams in Fig. 1 cancel in exactly the same way as the diagrams which, by power counting, could give a hard thermal loop 4-point function. In particular, this means that the large contributions in an Abelian theory cancel even at a given loop order, i.e., to see this cancellation no resummation is necessary ⁶.

In contrast, in a non-Abelian theory, there are hard thermal loop n -point functions for all n . Thus in non-Abelian theories this cancellation does not occur.

4 One-loop polarization tensor within the hard thermal loop effective theory

From the discussion in the previous section it should be clear that the calculation of the diagrams in Fig. 1 become simpler, if one uses the hard thermal loop effective theory. Then they correspond to a single diagram, which is shown in Fig. 2(a).

The spatial loop momenta within the hard thermal loop effective theory should be smaller than Λ , where

$$gT \ll \Lambda \ll T. \quad (4.1)$$

We also introduce a scale μ , which separates soft momenta from momenta of order gT , such that

$$g^2T \ll \mu \ll gT. \quad (4.2)$$

⁶The cancellation at fixed loop order has already been noticed in Ref. [19].

We consider only loop momenta larger than μ , which yields an effective theory for momenta smaller than μ .

In addition to the propagator (2.7), we will need the expressions for hard thermal loop 3- and 4-point functions. They are easily obtained from a generating functional like the one given in Ref. [20] (for other representations of the hard thermal loop effective action, see [21, 22]). The n -point vertex can be written as

$$\begin{aligned} \delta\Gamma_{\mu_1 \dots \mu_n}^{a_1 \dots a_n}(P_1, \dots, P_n) &= g^{n-2} m_D^2 \int \frac{d\Omega_{\mathbf{v}}}{4\pi} v_{\mu_1} \dots v_{\mu_n} \frac{1}{v \cdot P_n} \\ &\left\{ 2 \operatorname{tr}(T^{a_n} [T^{a_{n-1}}, [\dots, T^{a_1}] \dots]) \frac{p_1^0}{v \cdot P_1} \frac{1}{v \cdot (P_1 + P_2)} \dots \frac{1}{v \cdot (P_1 + \dots + P_{n-2})} \right. \\ &\quad \left. + \text{permutations}[(P_1, a_1), \dots, (P_{n-1}, a_{n-1})] \right\}, \end{aligned} \quad (4.3)$$

where T^a are the $SU(N)$ generators in the fundamental representation, normalized such that $\operatorname{tr}(T^a T^b) = (1/2)\delta^{ab}$.

We use the imaginary time formalism [23]. After the sum over Matsubara frequencies has been performed, one can analytically continue the external p_0 towards the real axis.

4.1 Diagram 2a

With the expression for the hard thermal loop 4-point function taken from Eq. (4.3), one finds

$$\Pi_{\mu\nu}^{(2a)}(P) = m_D^2 N g^2 \int \frac{d\Omega_{\mathbf{v}}}{4\pi} \frac{v_\mu v_\nu v_\rho v_\sigma}{(v \cdot P)^2} \not\sum_K \left[\frac{k_0 + p_0}{v \cdot (K + P)} - \frac{k_0}{v \cdot K} \right] \Delta^{\rho\sigma}(K), \quad (4.4)$$

where

$$\not\sum_K f(K) \equiv T \sum_{k_0=i\omega_n} \int \frac{d^3k}{(2\pi)^3} f(K), \quad (4.5)$$

and $\omega_n = 2\pi nT$ are the Matsubara frequencies with integer n running from $-\infty$ to $+\infty$.

Performing the frequency sum can be quite tedious. One method, which turns out to be quite convenient in the present case, is described in Appendix A. In order to make use of Eq. (A.6), we rewrite the sum appearing in (4.4)

$$S \equiv \not\sum_K \left[\frac{k_0 + p_0}{v \cdot (K + P)} - \frac{k_0}{v \cdot K} \right] \Delta^{\rho\sigma}(K), \quad (4.6)$$

as

$$S = -\frac{1}{2} \not\sum_K \left[\frac{k_0 + p_0}{v \cdot (K + P)} - \frac{k_0}{v \cdot K} \right] [\Delta^{\rho\sigma}(K + P) - \Delta^{\rho\sigma}(K)]. \quad (4.7)$$

Now we apply Eq. (A.6) to obtain

$$S \simeq -\frac{1}{2}T p_0 \int \frac{d^3k}{(2\pi)^3} \quad (4.8)$$

$$\left\{ \frac{\Delta^{\rho\sigma}(p_0, \mathbf{k} + \mathbf{p}) - \Delta^{\rho\sigma}(0, \mathbf{k})}{v \cdot P - \mathbf{v} \cdot \mathbf{k}} + \frac{\Delta^{\rho\sigma}(0, \mathbf{k} + \mathbf{p}) - \Delta^{\rho\sigma}(-p_0, \mathbf{k})}{-p_0 - \mathbf{v} \cdot \mathbf{k}} \right.$$

$$\left. - \int \frac{dk_0}{2\pi i} \frac{\Delta^{\rho\sigma}(K + \frac{1}{2}P) - \Delta^{\rho\sigma}(K - \frac{1}{2}P)}{(k_0 + \frac{1}{2}p_0)(k_0 - \frac{1}{2}p_0)} \left[\frac{k_0 + \frac{1}{2}p_0}{v \cdot (K + \frac{1}{2}P)} - \frac{k_0 - \frac{1}{2}p_0}{v \cdot (K - \frac{1}{2}P)} \right] \right\}.$$

In this expression the analytic continuation of p_0 away from Matsubara frequencies has already been performed. Furthermore, the high temperature approximation for the Bose distribution function has been used.

Eq. (4.8) looks quite complicated. However, in the case, we are interested in, which is $P \sim g^2T$, $K \sim gT$, it can be simplified considerably. Inside the integrand one can set $P = 0$ except for the imaginary part of p_0 . The error made with this approximation is of order g . Then, the first two terms in the curly bracket vanish, and one obtains

$$\Pi_{\mu\nu}^{(2a)}(P) \simeq -\frac{i}{2}m_{\text{D}}^2 N g^2 T p_0 \int \frac{d\Omega_{\mathbf{v}}}{4\pi} \frac{v_{\mu}v_{\nu}v_{\rho}v_{\sigma}}{(v \cdot P)^2} \int \frac{d^4k}{(2\pi)^4} \frac{1}{k_0} \text{disc}(\Delta^{\rho\sigma}(K)) \text{disc}\left(\frac{1}{v \cdot K}\right). \quad (4.9)$$

Eq. (4.9) is gauge fixing independent in covariant gauges. The terms proportional to the gauge fixing parameter ξ contain factors $v \cdot K$, which vanish due to

$$\text{disc}\left(\frac{1}{v \cdot K}\right) = -i2\pi\delta(v \cdot K). \quad (4.10)$$

Note that $v \cdot K = 0$ is the approximate on-shell condition for the loop momentum $Q + P$ in Fig. 1. In this case we have

$$(v\mathcal{P}_{\text{t}}(\mathbf{k})v) = -(v\mathcal{P}_{\ell}(K)v) = 1 - \frac{k_0^2}{k^2} \quad (v \cdot K = 0), \quad (4.11)$$

so that

$$\Pi_{\mu\nu}^{(2a)}(P) \simeq -\frac{i}{2}m_{\text{D}}^2 N g^2 T p_0 \int \frac{d\Omega_{\mathbf{v}}}{4\pi} \frac{v_{\mu}v_{\nu}}{(v \cdot P)^2}$$

$$\int \frac{d^4k}{(2\pi)^4} \frac{1}{k_0} \left(1 - \frac{k_0^2}{k^2}\right) \text{disc}(\Delta_{\text{t}}(K) - \Delta_{\ell}(K)) \text{disc}\left(\frac{1}{v \cdot K}\right). \quad (4.12)$$

At this point one can see that $\Pi_{\mu\nu}^{(2a)}$ is insensitive to the UV cutoff Λ . Due to Eq. (4.10), only space-like momenta contribute to (4.12). Then, the only discontinuity of the propagators $\Delta_{\text{t},\ell}$ is due to the discontinuity of the selfenergies,

$$\text{disc}(\Delta_{\text{t},\ell}(K)) = -|\Delta_{\text{t},\ell}(K)|^2 \text{disc}(\delta\Pi_{\text{t},\ell}(K)) \quad (K^2 < 0), \quad (4.13)$$

which falls off like $1/k^4$ for $k \gg m_{\text{D}}$.

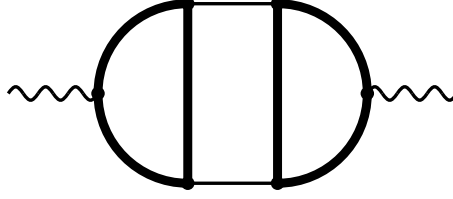


Figure 3: Ladder-type diagram with two hard loop integrations corresponding to the effective diagram in Fig. 2(b). The notation is the same as in Fig. 1.

However, the part containing the transverse propagator is sensitive to the IR cutoff μ , because $\Delta_t(K)$ is unscreened for $k_0 \ll k$. To compute the μ -dependent piece of (4.12), one can use the small frequency approximation (2.11) for $\Delta_t(K)$ and neglect k_0 relative to k otherwise. Then the delta-function in Eq. (4.10) becomes $\delta(\mathbf{v} \cdot \mathbf{k})$, and one obtains

$$\Pi_{\mu\nu}^{(2a)}(P) \simeq -\frac{i}{4\pi} m_D^2 N g^2 T p_0 \int \frac{d\Omega_{\mathbf{v}}}{4\pi} \frac{v_\mu v_\nu}{(v \cdot P)^2} \left[\log \left(\frac{gT}{\mu} \right) + \text{finite} \right], \quad (4.14)$$

where “finite” denotes terms which are IR finite, i.e., which are not sensitive to μ . The finite terms depend on how exactly the cutoff is implemented.

4.2 Diagram 2b

The result (4.14) is gauge fixing independent, but it is not transverse. There is, however, another one-loop diagram in the hard thermal loop effective theory, which contributes at the same order (Fig. 2(b))⁷. In the original theory it corresponds to a 3-loop diagram with two hard loop momenta (Fig. 3). The vertices can be read off from Eq. (4.4), and one obtains

$$\begin{aligned} \Pi_{\mu\nu}^{(2b)}(P) &= -\frac{1}{2} m_D^4 N g^2 \int \frac{d\Omega_{\mathbf{v}_1}}{4\pi} \frac{v_{1\mu} v_{1\rho} v_{1\sigma}}{v_1 \cdot P} \int \frac{d\Omega_{\mathbf{v}_2}}{4\pi} \frac{v_{2\nu} v_{2\tau} v_{2\lambda}}{v_2 \cdot P} \\ &\quad \sum_K \Delta^{\rho\tau}(K) \Delta^{\sigma\lambda}(K+P) \left[\frac{k_0}{v_1 \cdot K} - \frac{k_0 + p_0}{v_1 \cdot (K+P)} \right] \left[\frac{k_0}{v_2 \cdot K} - \frac{k_0 + p_0}{v_2 \cdot (K+P)} \right]. \end{aligned} \quad (4.15)$$

Again, we use Eq. (A.6) to perform the sum over Matsubara frequencies, and the terms $f(0, p_0)$, $f(p_0, p_0)$ in (A.6) do not contribute at leading order in g . We neglect P relative to K except for the imaginary part of p_0 (see below), which gives

$$\Pi_{\mu\nu}^{(2b)}(P) \simeq -\frac{i}{2} m_D^4 N g^2 T p_0 \int \frac{d\Omega_{\mathbf{v}_1}}{4\pi} \frac{v_{1\mu} v_{1\rho} v_{1\sigma}}{v_1 \cdot P} \int \frac{d\Omega_{\mathbf{v}_2}}{4\pi} \frac{v_{2\nu} v_{2\tau} v_{2\lambda}}{v_2 \cdot P} \quad (4.16)$$

⁷The diagrams in Fig. 2 have been evaluated previously on the plasmon “mass shell” of the propagators (2.8) to compute the gluon damping rate [24] and corrections to the longitudinal plasmon frequency [25]. Our result does not apply to this case since we consider $p_0 \ll gT$.

$$\int \frac{d^4 k}{(2\pi)^4} \Delta^{\rho\tau}(k_0 - i\epsilon, \mathbf{k}) \Delta^{\sigma\lambda}(k_0 + i\epsilon, \mathbf{k}) \text{disc} \left(\frac{1}{v_1 \cdot K} \right) \text{disc} \left(\frac{1}{v_2 \cdot K} \right).$$

Due to the delta-functions $\delta(v_i \cdot K)$, only space-like K contribute in Eq. (4.16). Thus, there is no contribution from the plasmon poles of the propagators at $k_0^2 = \omega_{t,\ell}^2(k) > k^2$, which means that large denominators as in Eq. (2.1) cannot arise here. Therefore, it was consistent to neglect P in the propagators.

Now we insert the expression for the propagator (2.7). Again, the terms proportional to the gauge fixing parameter ξ drop out due to the delta functions $\delta(v \cdot K)$. Thus, we find that also the leading order contribution from diagram 2(b) is gauge fixing independent. The remaining terms give

$$\begin{aligned} \Pi_{\mu\nu}^{(2b)}(P) &\simeq -\frac{i}{2} m_D^4 N g^2 T p_0 \int \frac{d\Omega_{\mathbf{v}_1}}{4\pi} \frac{v_{1\mu}}{v_1 \cdot P} \int \frac{d\Omega_{\mathbf{v}_2}}{4\pi} \frac{v_{2\nu}}{v_2 \cdot P} \\ &\int \frac{d^4 k}{(2\pi)^4} \left| (v_1 \mathcal{P}_t v_2) \Delta_t(K) + (v_1 \mathcal{P}_\ell v_2) \Delta_\ell(K) \right|^2 \text{disc} \left(\frac{1}{v_1 \cdot K} \right) \text{disc} \left(\frac{1}{v_2 \cdot K} \right). \end{aligned} \quad (4.17)$$

It is now easy to see that the K -integral is insensitive to Λ , for $k \gg gT$ the propagators fall off like $1/k^2$. Note that this integral also appears in the collision term in the Boltzmann equation of Refs. [12, 15]. There, the integrand is given by the square of an on-shell matrix element.

Again, there is an infrared sensitive piece in the K -integral, which is due to the term containing $|\Delta_t(K)|^2$. To compute this piece, one can use the small frequency approximation (2.11) for $\Delta_t(K)$, and one can neglect k_0 otherwise. Using

$$\int d\Omega_{\mathbf{k}} (v_1 \mathcal{P}_t v_2)^2 \delta(\mathbf{v}_1 \cdot \mathbf{k}) \delta(\mathbf{v}_2 \cdot \mathbf{k}) = \frac{2}{k^2} \frac{(\mathbf{v}_1 \cdot \mathbf{v}_2)^2}{\sqrt{1 - (\mathbf{v}_1 \cdot \mathbf{v}_2)^2}} \Theta(-K^2), \quad (4.18)$$

one finds

$$\begin{aligned} \Pi_{\mu\nu}^{(2b)}(P) &\simeq \frac{i}{\pi^2} m_D^2 N g^2 T p_0 \int \frac{d\Omega_{\mathbf{v}_1}}{4\pi} \frac{v_{1\mu}}{v_1 \cdot P} \int \frac{d\Omega_{\mathbf{v}_2}}{4\pi} \frac{v_{2\nu}}{v_2 \cdot P} \\ &\left[\log \left(\frac{gT}{\mu} \right) \frac{(\mathbf{v}_1 \cdot \mathbf{v}_2)^2}{\sqrt{1 - (\mathbf{v}_1 \cdot \mathbf{v}_2)^2}} + \text{finite} \right]. \end{aligned} \quad (4.19)$$

4.3 Diagrams containing tree level vertices

So far we have considered diagrams, which contain only hard thermal loop vertices. Now we will see that diagrams containing tree level vertices are smaller by one power of g .

The diagrams containing *only* tree level vertices have already been discussed in Ref. [7]. They are quite similar to hard thermal loops since the loop momentum is

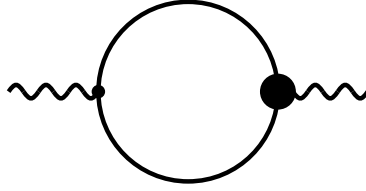


Figure 4: Sub-leading contribution to the one-loop polarization tensor with one hard thermal loop vertex and one tree level vertex. The notation is the same as in Fig. 2.

large compared to the external momentum. The size of hard thermal loops is determined by integrals like

$$\int_{\Lambda}^{\infty} dk k n(k) \sim T^2. \quad (4.20)$$

In our case, k is smaller than Λ , which means that one can approximate $n(k) \simeq T/k$. Thus, instead of (4.20), we have

$$\int_{\mu}^{\Lambda} dk k \frac{T}{k}. \quad (4.21)$$

The integration region $k \sim gT$ gives a contribution which is smaller than the hard thermal loop by one power of g . From k near the cutoff Λ , one obtains a contribution which cancels the Λ -dependence of the integral (4.20)⁸.

Now consider the diagram with one hard thermal loop and one tree level vertex in Fig. 4, which gives

$$\begin{aligned} \Pi_{\mu\nu}^{(4)}(P) &= -\frac{i}{2} m_D^2 N g \int \frac{d\Omega_{\mathbf{v}}}{4\pi} \frac{v_{\mu} v_{\rho} v_{\sigma}}{v \cdot P} \\ &\sum_K^f \Delta^{\rho\tau}(K) \Delta^{\sigma\lambda}(K+P) \Gamma_{\nu\lambda\tau}(-P, K+P, -K) \left[\frac{k_0}{v \cdot K} - \frac{k_0 + p_0}{v \cdot (K+P)} \right], \end{aligned} \quad (4.22)$$

where Γ is the tree level vertex. After performing the frequency sum, the square bracket gives a factor $\delta(v \cdot K)$ in the $P \rightarrow 0$ limit. Thus, there are only contributions from space-like K and one can also take the limit $P \rightarrow 0$ in the propagators. Since (4.22) contains only a single factor $1/v \cdot P$, rather than two, it is suppressed relative to (4.14), (4.19) by a factor g .

⁸The difficulties with this cancellation which were encountered in Ref. [26] are irrelevant as long as one does perturbation theory.

4.4 The logarithmic approximation

Keeping only the terms in Eqs. (4.14), (4.19), which depend logarithmically on μ , the polarization tensor becomes [11]

$$\Pi_{\mu\nu}^{(\text{LA})}(P) = im_D^2 N g^2 T \log\left(\frac{gT}{\mu}\right) p_0 \int \frac{d\Omega_{\mathbf{v}_1}}{4\pi} \frac{v_{1\mu}}{v_1 \cdot P} \int \frac{d\Omega_{\mathbf{v}_2}}{4\pi} \frac{v_{2\nu}}{v_2 \cdot P} I(\mathbf{v}_1, \mathbf{v}_2). \quad (4.23)$$

Here, the function

$$I(\mathbf{v}_1, \mathbf{v}_2) \equiv -\delta^{(S^2)}(\mathbf{v}_1 - \mathbf{v}_2) + \frac{1}{\pi^2} \frac{(\mathbf{v}_1 \cdot \mathbf{v}_2)^2}{\sqrt{1 - (\mathbf{v}_1 \cdot \mathbf{v}_2)^2}} \quad (4.24)$$

is the same as the one which appears in the noise correlator and in the collision term in the Boltzmann equation of Ref. [7]. Furthermore, $\delta^{(S^2)}$ is the delta-function on the two dimensional unit sphere,

$$\int d\Omega_{\mathbf{v}_1} f(\mathbf{v}_1) \delta^{(S^2)}(\mathbf{v} - \mathbf{v}_1) = f(\mathbf{v}). \quad (4.25)$$

One can easily verify that

$$\int d\Omega_{\mathbf{v}_1} I(\mathbf{v}_1, \mathbf{v}_2) = 0. \quad (4.26)$$

This implies that the polarization tensor (4.23) is transverse with respect to the external 4-momentum,

$$p^\mu \Pi_{\mu\nu}^{(\text{LA})}(P) = 0. \quad (4.27)$$

This condition is necessary for the effective theory for the soft fields to be gauge invariant.

4.5 Beyond the logarithmic approximation

In the previous section we found that the leading logarithmic result for the polarization tensor is transverse. Now we will see that this result holds beyond the leading logarithmic approximation, i.e., at leading order in g .

In order to define $\Pi_{\mu\nu}$ beyond the logarithmic approximation, one has to specify the way how the loop momenta are cut off in the infrared. A convenient method is dimensional regularization. Then, the above calculation of $\Pi_{\mu\nu}$ has to be repeated in $n = 4 - 2\varepsilon$ instead of 4 dimensions, which is straightforward. In the hard thermal loop selfenergies and vertices, the angular integration $\int d\Omega(\dots)$ become $n - 2$ dimensional, and in Eqs. (2.2), (4.3) one has to replace

$$\int \frac{d\Omega_{\mathbf{v}}}{4\pi} \rightarrow \int \frac{d\Omega_{\mathbf{v}}}{\Omega}, \quad (4.28)$$

where $\Omega = \int d\Omega$. Furthermore, one has to introduce a scale $\bar{\mu}$ in order to keep the coupling constant dimensionless.

Then, the polarization tensor can be written as

$$\Pi_{\mu\nu}(P) = im_{\text{D}}^2 N g^2 \bar{\mu}^{2\varepsilon} T p_0 \int \frac{d\Omega_{\mathbf{v}_1}}{\Omega} \frac{v_{1\mu}}{v_1 \cdot P} \int \frac{d\Omega_{\mathbf{v}_2}}{\Omega} \frac{v_{2\nu}}{v_2 \cdot P} \bar{I}(\mathbf{v}_1, \mathbf{v}_2), \quad (4.29)$$

where

$$\begin{aligned} \bar{I}(\mathbf{v}_1, \mathbf{v}_2) &= -\frac{1}{2} \int \frac{d^n k}{(2\pi)^n} \\ &\left\{ \Omega \delta^{(S^{n-2})}(\mathbf{v}_1 - \mathbf{v}_2) \frac{1}{k_0} \left(1 - \frac{k_0^2}{k^2}\right) \text{disc}[\Delta_{\text{t}}(K) - \Delta_{\ell}(K)] \text{disc}\left(\frac{1}{v_1 \cdot K}\right) \right. \\ &\left. + m_{\text{D}}^2 \left| (v_1 \mathcal{P}_{\text{t}} v_2) \Delta_{\text{t}}(K) + (v_1 \mathcal{P}_{\ell} v_2) \Delta_{\ell}(K) \right|^2 \text{disc}\left(\frac{1}{v_1 \cdot K}\right) \text{disc}\left(\frac{1}{v_2 \cdot K}\right) \right\}. \end{aligned} \quad (4.30)$$

We will now see, that $\bar{I}(\mathbf{v}_1, \mathbf{v}_2)$ also satisfies (4.26), which then implies that Π in Eq. (4.29) is transverse. We have

$$\begin{aligned} \int \frac{d\Omega_{\mathbf{v}_1}}{\Omega} \bar{I}(\mathbf{v}_1, \mathbf{v}_2) &= -\frac{1}{2} \int \frac{d^n k}{(2\pi)^n} \text{disc}\left(\frac{1}{v_2 \cdot K}\right) \\ &\left\{ \frac{1}{k_0} \left(1 - \frac{k_0^2}{k^2}\right) \text{disc}[\Delta_{\text{t}}(K) - \Delta_{\ell}(K)] \right. \\ &\left. + m_{\text{D}}^2 \int \frac{d\Omega_{\mathbf{v}_1}}{\Omega} \left| (v_1 \mathcal{P}_{\text{t}} v_2) \Delta_{\text{t}}(K) + (v_1 \mathcal{P}_{\ell} v_2) \Delta_{\ell}(K) \right|^2 \text{disc}\left(\frac{1}{v_1 \cdot K}\right) \right\}. \end{aligned} \quad (4.31)$$

For the first term in the curly bracket one can use Eq. (4.13) to write the discontinuities of the propagators in terms of the discontinuities of the corresponding selfenergies. The latter can be read off from (the n -dimensional version of) Eq. (2.2) making use of the projectors (2.4), (2.5). Taking into account that, in n dimensions, $\mathcal{P}_{\text{t}}^{ii} = n - 2$, one finds

$$\begin{aligned} \text{disc}[\Delta_{\text{t}}(K) - \Delta_{\ell}(K)] &= -m_{\text{D}}^2 k_0 \left(1 - \frac{k_0^2}{k^2}\right) \left[\frac{1}{n-2} |\Delta_{\text{t}}(K)|^2 + |\Delta_{\ell}(K)|^2 \right] \\ &\int \frac{d\Omega_{\mathbf{v}_1}}{\Omega} \text{disc}\left(\frac{1}{v_1 \cdot K}\right), \end{aligned} \quad (4.32)$$

which contains precisely the same $\Omega_{\mathbf{v}_1}$ -integral as the second term in the curly bracket of Eq. (4.31).

In the second term in the curly bracket of Eq. (4.31) we can perform the angular integration over \mathbf{v}_1 . Due to $v_1 \cdot K = v_2 \cdot K = 0$, the velocity vectors can be written as

$$\mathbf{v}_i = \frac{k_0}{k} \hat{\mathbf{k}} + \sqrt{1 - \frac{k_0^2}{k^2}} \hat{\varphi}_i \quad (i = 1, 2), \quad (4.33)$$

where $\hat{\varphi}_i$ are unit vectors orthogonal to $\hat{\mathbf{k}} = \mathbf{k}/k$. Then we have

$$(v_1 \mathcal{P}_t v_2) = \left(1 - \frac{k_0^2}{k^2}\right) \hat{\varphi}_1 \cdot \hat{\varphi}_2, \quad (4.34)$$

$$(v_1 \mathcal{P}_\ell v_2) = -1 + \frac{k_0^2}{k^2}. \quad (4.35)$$

Now one can perform the $\hat{\varphi}_1$ -integration. The transverse-longitudinal interference term in Eq. (4.31) vanishes due to

$$\int d\hat{\varphi}_1 \hat{\varphi}_1 \cdot \hat{\varphi}_2 = 0. \quad (4.36)$$

Furthermore, we have

$$\int d\hat{\varphi}_1 (\hat{\varphi}_1 \cdot \hat{\varphi}_2)^2 = \frac{1}{n-2} \Omega. \quad (4.37)$$

Consequently, for $v_2 \cdot K = 0$, one can write

$$\begin{aligned} \int \frac{d\Omega_{\mathbf{v}_1}}{\Omega} \left| (v_1 \mathcal{P}_t v_2) \Delta_t(K) + (v_1 \mathcal{P}_\ell v_2) \Delta_\ell(K) \right|^2 \text{disc} \left(\frac{1}{v_1 \cdot K} \right) = \\ \left(1 - \frac{k_0^2}{k^2}\right)^2 \int \frac{d\Omega_{\mathbf{v}_1}}{\Omega} \left[\frac{1}{n-2} |\Delta_t(K)|^2 + |\Delta_\ell(K)|^2 \right] \text{disc} \left(\frac{1}{v_1 \cdot K} \right). \end{aligned} \quad (4.38)$$

Inserting Eqs. (4.32), (4.38) into (4.31), one finds that the two terms in the curly bracket cancel, and consequently

$$\int d\Omega_{\mathbf{v}_1} \bar{I}(\mathbf{v}_1, \mathbf{v}_2) = 0. \quad (4.39)$$

This implies that Π in Eq. (4.29) is transverse with respect to the external n -momentum,

$$p^\mu \Pi_{\mu\nu}(P) = 0. \quad (4.40)$$

5 Summary and Discussion

We have seen that in non-Abelian gauge theories the hard thermal loop approximation is not sufficient for obtaining the effective theory for soft momentum fields. When $p_0 \lesssim g^2 T$, the polarization tensor for soft external momenta receives higher loop contributions from loop momenta larger than $g^2 T$, which are as large as the hard thermal loops.

These large higher loop contributions are due to ladder type diagrams and diagrams with selfenergy insertions on propagators carrying hard momenta. Their calculation is simplified if it is performed in two steps. First, one integrates out the hard momenta,

which gives the well known hard thermal loop effective theory for momenta $p \ll T$. Then, the polarization tensor is calculated within this effective theory by integrating over momenta of order gT . When the calculation is organized in this way, it is easy to see why these large contributions cancel in an Abelian theory. The large contributions discussed in this paper contain only hard thermal loop gauge field vertices, which are absent in the Abelian case.

The calculation of the one-loop polarization tensor in the hard thermal loop effective theory requires an explicit IR cutoff separating spatial momenta of order g^2T from momenta of order gT . We have obtained an expression for the polarization tensor valid to leading order in g . It is gauge fixing independent in covariant gauges and Coulomb-like gauges. Furthermore, it is transverse with respect to the external 4-momentum, which is necessary for the resulting effective theory to be gauge invariant. The dependence on the cutoff is logarithmic, and the cutoff dependent part was computed explicitly.

In the physically interesting region of very small frequencies $p_0 \ll g^2T$, only the 3-d transverse part of the polarization tensor is unsuppressed relative to the hard thermal loop $\delta\Pi_t$. The longitudinal part is small compared to $\delta\Pi_\ell$, which, in the small frequency limit, approximately equals m_D^2 .

The discussion was restricted to one-loop diagrams in the hard thermal loop effective theory, corresponding to 2- and 3-loop diagrams in the original theory. Analyzing higher loop diagrams is quite tedious, even in the present framework. It is a lot more convenient [7] to use the formulation of the hard thermal loop effective theory in terms of classical kinetic equations. In this approach it is straightforward to resum all leading logarithmic contributions from higher loop diagrams. Integrating out the scale gT generates a Gaussian noise term and a collision term in the equations of motion for the soft field modes (see also [12]-[15]), where the noise correlator and the integral kernel of the collision term are proportional to (4.24).⁹

Acknowledgments. I am grateful to Peter Arnold, Mikko Laine, Bert-Jan Nauta, and Toni Rebhan for useful discussions and comments, and to Kimmo Kainulainen and Kari Rummukainen for critical comments on the manuscript. This work was supported in part by the TMR network “Finite temperature phase transitions in particle physics”, EU contract no. ERBFMRXCT97-0122.

⁹In scalar field theory the summation of ladder diagrams also leads to a Boltzmann equation containing a collision term [27].

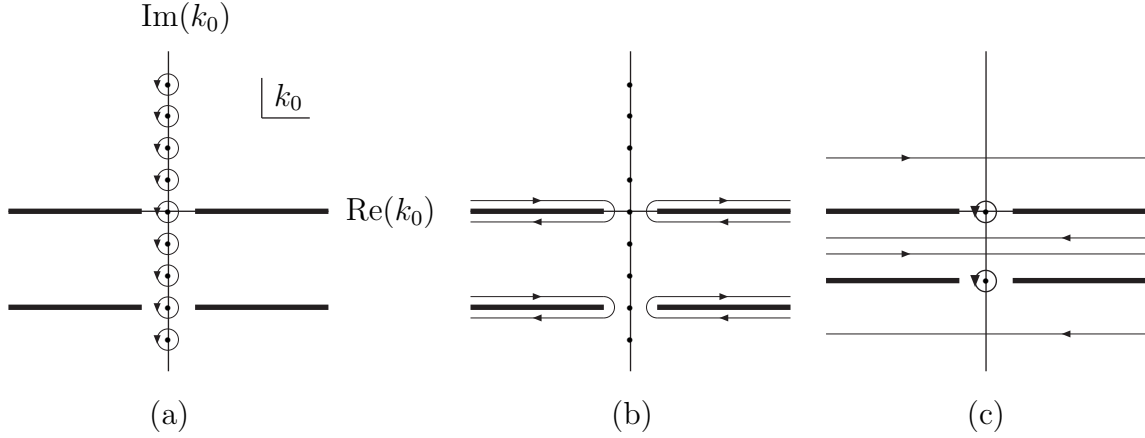


Figure 5: Integration contours in the complex k_0 plane for the integrals in (a) Eq. (A.2) and (b) Eq. (A.3). The contour in (c) corresponds to the integral in Eq. (A.6). The lowest and highest branches can be moved to $\pm i\infty$ and do not contribute. The thick lines are the cuts of the function $f(k_0, p_0)$ located at $\text{Im}(k_0) = 0$ and $\text{Im}(k_0) = -\text{Im}(p_0)$.

Appendix A

For diagrams containing the hard thermal loop resummed propagators, the sum over Matsubara frequencies is not easy to compute. The standard method [23] is to write the propagators in their spectral representations. This method is not always useful. In particular, for the diagram in Fig. 2b it turns out to be very inconvenient. This Appendix describes an alternative method, which is very efficient when applied to the diagrams considered in Sect. 4.

The sums are of the form

$$S = T \sum_{k_0=i\omega_n} f(k_0, p_0), \quad (\text{A.1})$$

where $p_0 = i\omega_{n'}$ is a Matsubara frequency. For given p_0 , the function $f(k_0, p_0)$ has cuts in the complex k_0 plane for $\text{Im}(k_0) = 0$ and for $\text{Im}(k_0) = -p_0$ (Fig. 5).

First we write the sum as an integral along the contour C_a depicted in Fig. 5(a)

$$S = \int_{C_a} \frac{dk_0}{2\pi i} \left(\frac{1}{2} + n(k_0) \right) f(k_0, p_0), \quad (\text{A.2})$$

where $n(k_0)$ is the Bose distribution function (3.1). Then the contour is deformed as in Fig. 5(b), which gives

$$S = \int \frac{dk_0}{2\pi i} \left(\frac{1}{2} + n(k_0) \right) \left(f(k_0 + i\delta, p_0) - f(k_0 - i\delta, p_0) \right)$$

$$+ \int \frac{dk_0}{2\pi i} \left(\frac{1}{2} + n(k_0) \right) \left(f(k_0 - p_0 + i\delta, p_0) - f(k_0 - p_0 - i\delta, p_0) \right). \quad (\text{A.3})$$

Here the first (second) line corresponds to the upper (lower) part of the contour. In the second line we have used the periodicity of the function n , $n(k_0 + p_0) = n(k_0)$. Now we can perform the analytic continuation of p_0 to arbitrary complex values. We are interested in the case (2.9). The k_0 -integral is saturated for $|k_0| \ll T$ so that we can use the high temperature approximation

$$\frac{1}{2} + n(k_0) \simeq \frac{T}{k_0} \quad (\text{A.4})$$

to obtain

$$\begin{aligned} S \simeq & \int \frac{dk_0}{2\pi i} \frac{T}{k_0} \left(f(k_0 + i\delta, p_0) - f(k_0 - i\delta, p_0) \right) \\ & + \int \frac{dk_0}{2\pi i} \frac{T}{k_0} \left(f(k_0 - p_0 + i\delta, p_0) - f(k_0 - p_0 - i\delta, p_0) \right), \end{aligned} \quad (\text{A.5})$$

where $\delta < \text{Im}(p_0)$. Now we deform the integration contour as in Fig. 5(c): The upper part is closed around the pole at $k_0 = 0$. The piece above the cut can be moved towards $i \times \infty$ to give zero if $f(k_0, p_0)$ vanishes in this limit. The piece below the the cut is moved downwards to $\text{Im}(k_0) = -\text{Im}(p_0/2)$. Proceeding similarly for the lower part of the contour, we finally obtain

$$S \simeq T \left\{ f(0, p_0) + f(-p_0, p_0) - p_0 \int \frac{dk_0}{2\pi i} \frac{1}{k_0 + \frac{1}{2}p_0} \frac{1}{k_0 - \frac{1}{2}p_0} f(k_0 - \frac{1}{2}p_0, p_0) \right\}. \quad (\text{A.6})$$

Appendix B

In this Appendix it is shown that one obtains the same leading order result for the polarization tensor as in Sect. 4, if one uses Coulomb gauge rather than a covariant gauge.

In Coulomb-like gauges the hard thermal loop resummed propagator reads

$$\Delta^{\mu\nu} = \Delta_t \mathcal{P}_t^{\mu\nu} + \Delta_\ell \frac{K^2}{k^2} g^{\mu 0} g^{\nu 0} + \xi \frac{k^\mu k^\nu}{k^4}. \quad (\text{B.1})$$

Strict Coulomb gauge corresponds to $\xi \rightarrow 0$. In order to see the effect of using the propagator (B.1) instead of (2.7), it is convenient to write $g^{\mu 0} g^{\nu 0}$ in terms of the tensors (cf. Ref. [2]) $\mathcal{P}_\ell^{\mu\nu}$,

$$C^{\mu\nu} = \frac{1}{\sqrt{2}k} \left[\left(g^{\mu 0} - \frac{k^\mu k^0}{K^2} \right) k^\nu + \left(g^{\nu 0} - \frac{k^\nu k^0}{K^2} \right) k^\mu \right], \quad (\text{B.2})$$

and

$$D^{\mu\nu} = -\frac{k^\mu k^\nu}{K^2}. \quad (\text{B.3})$$

Using

$$\mathcal{P}_\ell D = 0, \quad \mathcal{P}_\ell^2 = -\mathcal{P}_\ell, \quad (\text{B.4})$$

and

$$\text{tr}(\mathcal{P}_\ell) = \text{tr}(D) = \text{tr}(C^2) = -1, \quad \text{tr}(C) = \text{tr}(\mathcal{P}_\ell C) = \text{tr}(CD) = 0, \quad (\text{B.5})$$

one finds

$$\Delta^{\mu\nu} = \Delta_t \mathcal{P}_t^{\mu\nu} + \Delta_\ell \left[\mathcal{P}_\ell^{\mu\nu} + \sqrt{2} \frac{k^0}{k} C^{\mu\nu} - \frac{k_0^2}{k^2} D^{\mu\nu} \right] + \xi \frac{k^\mu k^\nu}{k^4}. \quad (\text{B.6})$$

Now one can see that the propagator (B.6) gives the same result as the propagator (2.7). Each term in $C^{\mu\nu}$ and $D^{\mu\nu}$ contains at least one factor k^μ or k^ν , which will be contracted with some velocity vector v . Due to the delta functions $\delta(v \cdot K)$ all these terms vanish.

References

- [1] A. D. Linde, Phys. Lett. B 96 (1980) 289.
- [2] D. J. Gross, R. D. Pisarski and L. G. Yaffe, Rev. Mod. Phys. 53 (1981) 43.
- [3] K. Farakos, K. Kajantie, K. Rummukainen and M. Shaposhnikov, Nucl. Phys. B 425 (1994) 67; Nucl. Phys. B 442 (1995) 317; K. Kajantie, M. Laine, K. Rummukainen and M. Shaposhnikov, Nucl. Phys. B 458 (1996) 90; A. Jakovac, K. Kajantie and A. Patkos, Phys. Rev. D 49 (1994) 6810.
- [4] E. Braaten, A. Nieto, Phys. Rev. D 51 (1995) 6990.
- [5] For reviews of electroweak baryon number violation and electroweak baryogenesis, see A.G. Cohen, D.B. Kaplan, A.E. Nelson, Ann.Rev.Nucl.Part.Sci.43 (1993) 27, hep-ph/9302210; V.A. Rubakov, M. E. Shaposhnikov, Usp. Fis. Nauk 166 (1996) 493, hep-ph/9603208; A. Riotto, M. Trodden, CERN-TH-99-04, hep-ph/9901362.
- [6] S. Yu. Khlebnikov, M. E. Shaposhnikov, Nucl. Phys. **B308** (1988) 885.
- [7] D. Bödeker, Phys. Lett. B 426 (1998) 351.
- [8] G.D. Moore, MCGILL-98-28, hep-ph/9810313.
- [9] E. Braaten and R. Pisarski, Nucl. Phys. B 337 (1990) 569; J. Frenkel and J.C. Taylor, Nucl. Phys. B 334 (1990) 199.
- [10] P. Arnold, D. Son and L.G. Yaffe, Phys. Rev. D 55 (1997) 6264; P. Huet and D.T. Son, Phys. Lett. B 393 (1997) 94.
- [11] D. Bödeker, Proceedings of the *5th International Workshop on thermal field theories and their applications*, ed. U. Heinz, hep-ph/9811469.
- [12] P. Arnold, D. Son and L.G. Yaffe, UW/PT 98-10, MIT CTP-2779, hep-ph/9810216; UW/PT 98-11, hep-ph/9901304.
- [13] D. Litim, C. Manuel, ECM-UB-PF-99-04, CERN-TH-99-29, hep-ph/9902430.
- [14] M.A. Valle Basagoiti, EHU-FT/9905, hep-ph/9903462.
- [15] J. P. Blaizot, E. Iancu, Saclay-T99/026, CERN-TH/99-71, hep-ph/9903389.
- [16] See, e.g., H. A. Weldon, Phys. Rev. D 26 (1982) 1394.
- [17] V.V. Lebedev and A.V. Smilga, Physica A 181 (1992) 187.

- [18] M.E. Carrington, R. Kobes and E. Petitgirard, Phys. Rev. D 57 (1998) 2631.
- [19] M.E. Carrington and R. Kobes, Phys. Rev. D 57 (1998) 6372.
- [20] J. P. Blaizot, E. Iancu, Nucl.Phys. B 417 (1994) 608.
- [21] E. Braaten and R. Pisarski, Phys. Rev. D 45 (1992) 1827.
- [22] J.C. Taylor and S.M.H. Wong, Nucl. Phys. B 346 (1990) 115.
- [23] For a review, see M. Le Bellac, *Thermal field theory*, Cambridge University Press (1997).
- [24] E. Braaten and R. Pisarski, Phys. Rev. D 42 (1990) 2156.
- [25] H. Schulz, Nucl. Phys. B 413 (1994) 353.
- [26] D. Bödeker, L. McLerran and A.V. Smilga, Phys. Rev. D 52 (1995) 4675.
- [27] S. Jeon Phys. Rev. D 52 (1995) 3591; S. Jeon, L. G. Yaffe Phys. Rev. D 53 (1996) 5799.